Magnetically Induced Transparency and Its Application as an Accelerator

M.S. Hur*, J.S. Wurtele† and G. Shvets**

*University of California Berkeley
†University of California Berkeley and Lawrence Berkeley National Laboratory
**Illinois Institute of Technology

Abstract. Recently it was found [1-3] that a magnetized plasma can be made transparent to a right-hand polarized cyclotron frequency resonant wave in the presence of a strong pump or a helical magnetic wiggler. Theory predicts and simulations verify that the group velocity of the probe is slow, and the phase velocity of the longitudinal wave controllable. These properties of the system suggest the possibility of its being used as an advanced accelerator of heavy particles. We present the theory and simulations of transparency and a preliminary study of its application as an accelerator.

INTRODUCTION

Recently it was theoretically found that a magnetized plasma can be made transparent to a right-hand polarized wave (probe) at the cyclotron frequency in the presence of strong pump wave which is detuned by the plasma frequency [1-3]. This is a classical analogy of the quantum electromagnetically induced transparency (EIT) [4,5]. The basic idea is to cancel the resonant response of electrons to the probe by the sideband of pump induced by electron's ponderomotive motion. The same transparency can be induced by a static helical magnetically wiggler, where the wiggler replaces the dynamic magnetic field of the pump.

The wiggler-plasma system has numerous properties desirable for an heavy particle accelerator. The phase velocity of the longitudinal wave is slow, which makes it easier to trap non-relativistic heavy particles. Furthermore, the phase velocity is readily controlled by adjusting the wiggler wavelength.

THEORY AND SIMULATION

Figure 1 shows a schematics of the system. The plasma is magnetized by an axial magnetic field B_c. A right-hand polarized probe and pump are launched together, where the probe frequency is in cyclotron resonance and the pump frequency is down-shifted from the cyclotron resonance by the plasma frequency. When there is no pump, a large transverse current is resonantly excited and the probe is absorbed in the plasma. In the presence of the pump, electrons move longitudinally in the ponderomotive beat potential of the two waves, which varies as $e^{-i\Delta\omega t+i\Delta kz}$, where $\Delta\omega$ (Δk) is beat frequency (wavenumber) between the pump and the probe. The pump electric field as seen by

CP647, *Advanced Accelerator Concepts: Tenth Workshop*, edited by C. E. Clayton and P. Muggli

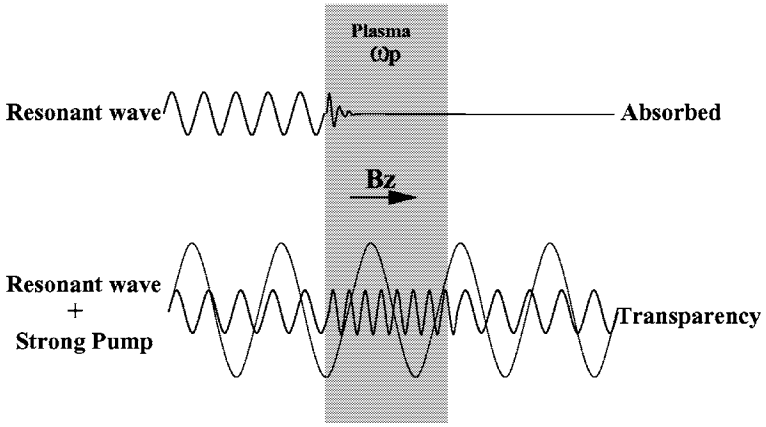

FIGURE 1. EIT in magnetized plasma

an electron is approximated as $\vec{E}_0(z,t) \simeq \vec{E}_0(z_0,t) + \zeta \times \partial_z \vec{E}_0$, where $z = z_0 + \zeta$, z_0 represents the initial position of the electron, and ζ is its longitudinal displacement. The second term couples the longitudinal motion and the transverse field, thereby inducing sidebands at frequencies $\omega_0 \pm \Delta\omega$. A critical aspect of induced transparency in plasma is that the electron perpendicular motion due to the probe electric field is canceled by the response to the upper sideband (which is at the probe frequency). Details of mathematical expansion can be found elsewhere [2,3], where it is shown that phase of the sideband field is automatically matched to cancel the probe field.

Transparency is demonstrated in Fig. 2. Parameters are probe intensity $a_1 = eE_1/mc^2k_1 = 0.005$, pump intensity $a_0 = 0.05$, $\omega_1 = \Omega_c$, $\omega_0 = 0.8\Omega_c$, and $\omega_p = (4\pi e^2 n_e/m)^{1/2} = 0.2\Omega_c$. The cyclotron frequency (Ω_c) is 1.8×10^{11} Hz. We measured the propagation of the wave envelope and the longitudinal wave inside the plasma slab. The oscillation pattern of the envelope is simply the beat of the pump and probe. At earlier times, in Fig. 2 (a), there is no beat on the right side of the plasma. This implies that the probe has not been transmitted. As the longitudinal wave is excited in the whole region of the plasma (Fig. 2 (d)), transparency of the probe is observed (Fig. 2 (c)).

The pump wave can be replaced by a helical magnetic wiggler with wavelength λ_w. In this case, the wiggler corresponds to a pump with zero frequency and wavenumber of $k_w = 2\pi/\lambda_w$. Therefore the matching condition for frequencies should be $\omega_p = \omega_1 - \omega_0 = \omega_1$. The longitudinal motion of an electron is

$$\zeta = \frac{\tilde{\zeta}}{2} e^{i\theta_1 \pm ik_w z_0} + \frac{\tilde{\zeta}^*}{2} e^{-i\theta_1 \mp ik_w z_0}, \tag{1}$$

where the signs $\pm$ represent right- and left-hand wiggler polarizations. The equation of transverse motion is

$$\dot{\beta}_+ + i\Omega_c \beta_+ = -\omega_1 a_1 e^{i\theta_1} + \frac{i\Omega_w}{c} \dot{\zeta} e^{\mp ik_w z_0}, \tag{2}$$

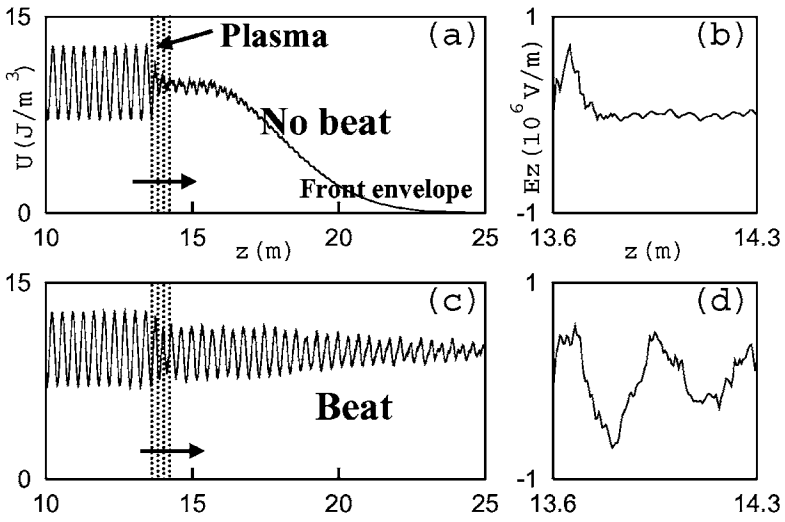

FIGURE 2. Simulation of resonant wave transparency. The wave envelope at two different times (left column) and the corresponding longitudinal wave inside the plasma slab (right column) shows that the excitation of the plasma wave leads to the transmission of the probe (see text).

where $\beta_+ = (v_x - iv_y)/2c$, $\theta_1 = ik_1 z_0 - i\omega_1 t$, and $\Omega_w = eB_w/mc$. A discussion of the polarization of the electron motion can be found in Ref. [3]. The eikonal term was approximated as $e^{ik_1(z_0+\zeta)-i\omega_1 t} \simeq e^{i\theta_1}(1+ik_1\zeta)$ and nonlinear terms in a_1 and ζ were ignored. Substituting Eq. (1) into Eq. (2) yields the steady-state solution for transverse motion:

$$\beta_+ = -\frac{i\omega_1}{\omega_1 - \Omega_c}(a_1 - \frac{\Omega_w}{2c}\tilde{\zeta})e^{i\theta_1} + \frac{i\omega_1\Omega_w}{2c(\omega_1+\Omega_c)}\tilde{\zeta}^* e^{-i\theta_1 \mp 2ik_w z}. \tag{3}$$

It is important to note that a finite solution can exist at resonance ($\omega_1 = \Omega_c$) when

$$a_1 = \frac{\Omega_w}{2c}\tilde{\zeta}. \tag{4}$$

Equation (4) represents the cancellation of probe by the probe-wiggler coupling.

A dispersion relation is obtained by considering the more general case of $\delta\Omega = \omega_1 - \Omega_c \neq 0$. To find $\tilde{\zeta}$ for a detuned probe, we solve the longitudinal equation of motion.

$$\ddot{\zeta} + \omega_p^2\zeta = -\frac{c^2}{2}k_1 a_1 \beta_+ e^{-i\theta_1} - \frac{i\Omega_w c}{2}(\beta_+ e^{\pm ik_w z_0}) + c.c. \tag{5}$$

The driving terms on the RHS of Eq. (5) are from $\vec{v}_\perp \times (\vec{B}_1 + \vec{B}_w)$ where $\vec{B}_1$ is the dynamic magnetic induction of the probe. Substituting Eq. (3) into Eq. (5) and using

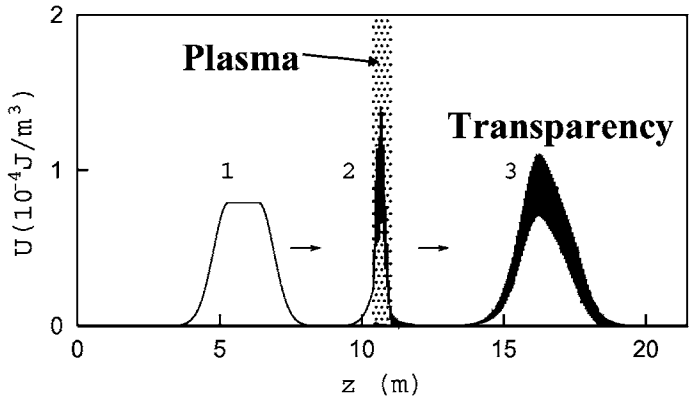

FIGURE 3. Simulation of transparency in a system where the pump electromagnetic wave is replaced by a wiggler field. The labels 1, 2, 3 refer to different times. Note that the pulse is compressed in the plasma.

$\partial_t^2 = -\omega_1^2$ yields

$$(-\omega_1^2 + \omega_p^2)\tilde{\xi} = c\Omega_w \left[\frac{\omega_1}{\omega_1 - \Omega_c} \left(a_1 - \frac{\Omega_w}{2c}\tilde{\xi} \right) - \frac{\Omega_w}{2c} \frac{\omega_1}{\omega_1 + \Omega_c} \tilde{\xi} \right]. \tag{6}$$

Eliminating $\tilde{\xi}$ from Eq. (3) and Eq. (6), the $e^{i\theta_1}$-component of β_+ is calculated as

$$\beta_+ = -i \frac{\omega_1 a_1 (\omega_1 \Omega_w^2 - 2(\Omega_c + \omega_1)^2 \delta\Omega)}{2\omega_1^2 \Omega_w^2 - 2(\Omega_c + \omega_1)^2 \delta\Omega^2} e^{i\theta_1}. \tag{7}$$

Using $-(c^2\partial_z^2 - \partial_t^2)E_1 = 4\pi\partial_t \vec{J}$ and the $e^{i\theta_1}$-component of $\vec{J}$ calculated from Eq. (7), the dispersion relation is derived:

$$\omega_1^2 = c^2 k_1^2 + \omega_1 \omega_p^2 \frac{\omega_1 \Omega_w^2 - 8\Omega_0^2 \delta\Omega}{2\omega_1^2 \Omega_w^2 - 8\Omega_0^2 \delta\Omega^2}. \tag{8}$$

Here only weak detuning ($\delta\Omega/\omega_1 \ll 1$) is considered and $O(\delta\Omega^3)$ were ignored.

Figure 3 is a simulation of probe transparency in the wiggler system. Since there is a large difference in the phase and group velocities, the pulse shape is distorted as it passes through the plasma.

A dispersion relation was obtained from simulations by measurement of wavelength as a function of frequency. Comparison with Eq. (8) is in Fig. 4. The theory and simulation are in good agreement except for the left-hand polarized wiggler with $\lambda_w =$ 0.3 m. We expect the difference in dispersion property between the left- and right-hand polarization of the wiggler originates from the second term on the RHS of Eq. (3). This term was ignored in the derivation of the dispersion relation, since it is generally not resonant with the $e^{i\theta_1}$-component of the probe. However at some specific values of λ_w, it

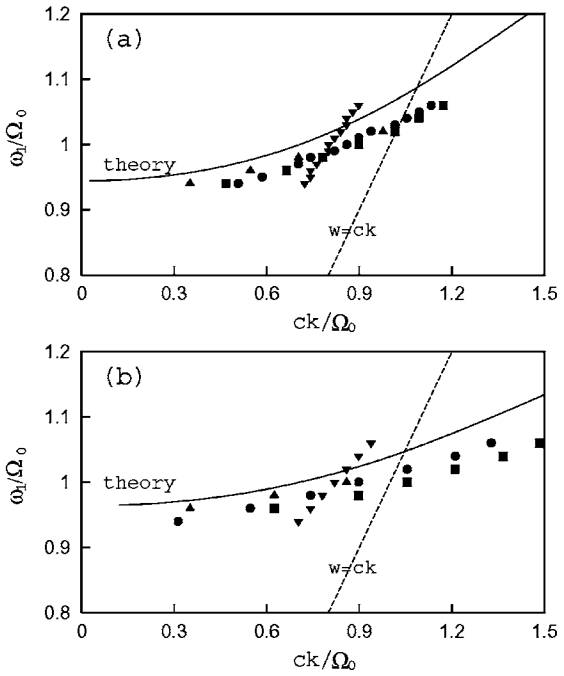

FIGURE 4. Dispersion relation of probe in wiggler system for (a) $B_w/B_c = 0.8$ and (b) $B_w/B_c = 0.6$. Wiggler parameters are a right-hand polarized wiggler with $\lambda_w = 0.3$ m (circles), left-hand with $\lambda_w = 0.3$ m (inverted triangles), right-hand with $\lambda_w = 0.1$ m (squares), and left-hand with $\lambda_w = 0.1$ m (triangles).

may become close to resonance or to a higher harmonic, in which case the theory should be modified to include the new term (this is currently under study).

INITIAL ACCELERATOR SIMULATIONS

One of the remarkable characteristics of the wiggler-plasma system is that the phase velocity of the longitudinal wave is readily controllable. This is possible since the longitudinal electron motion described by Eq. (1) gives a phase velocity $v_\phi = \omega_1/(k_w \pm k_1)$. The amplitude of the longitudinal wave does not depend on k_w. Therefore it is possible to control v_ϕ keeping the wave level fixed just by changing the wiggler wavelength. Since the wave level depends on ω_1, it is not a good parameter for controlling the phase velocity. The readily controllable phase velocity is a desirable property for an ion accelerator. Usually the ions or other heavy particles have low velocity, which requires low phase velocity for particle trapping. Figure 5 is an example of longitudinal electric field obtained from simulation for $a_1 = 0.04$, $B_c = 1$ T, $B_w = 0.7$ T, and $\lambda_w = 0.01$ m. The measured phase velocity is 0.5c which is very close to the theoretical value 0.56c. Theo-

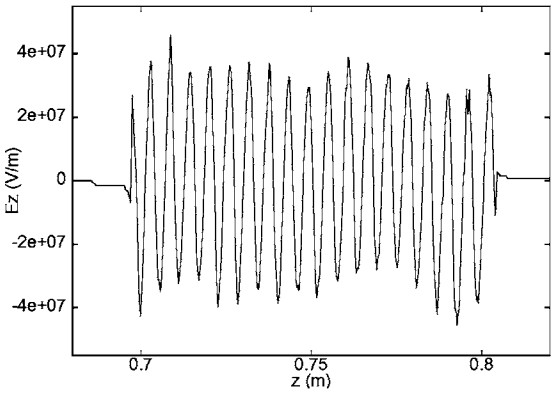

FIGURE 5. The longitudinal electric field for parameters $a_1 = 0.04$, $B_c = 1$ T, $B_w = 0.7$ T, and $\lambda_w = 0.01$ m.

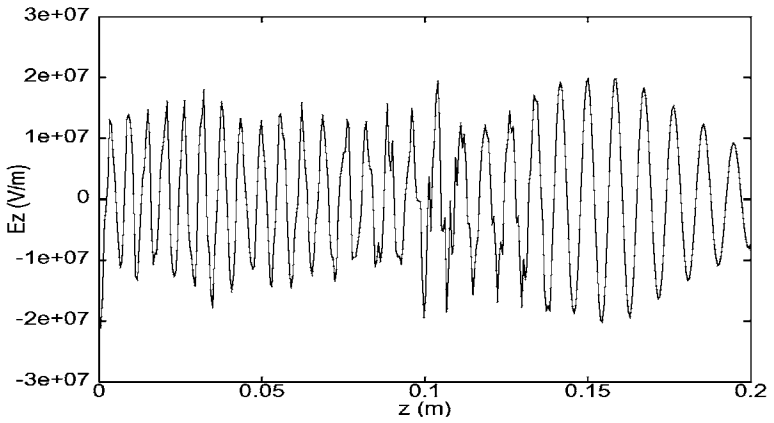

FIGURE 6. A tapered longitudinal wave for parameters $a_1 = 0.02$, $B_c = 1$ T, $B_w = 0.8$ T, and tapering $k_w(z) = 628 - 1250z$.

retically there is no limit in lowering down the phase velocity by decreasing the wiggler wavelength.

Spatial variation of the phase velocity is also possible by tapering the wiggler. This is very useful since it compensates for the drawback of using low phase velocity. The wavelength of the longitudinal wave should become shorter so as to make v_ϕ smaller (for a given frequency), but the particles accelerated on the short wavelength are prone to quick dephasing. The synchronism is maintained between the accelerating wave and the particles if the phase velocity increases as the particles are accelerated. Figure 6 is longitudinal electric field when a tapered wiggler was used. It is clearly seen that the wavelength becomes larger along the propagating direction.

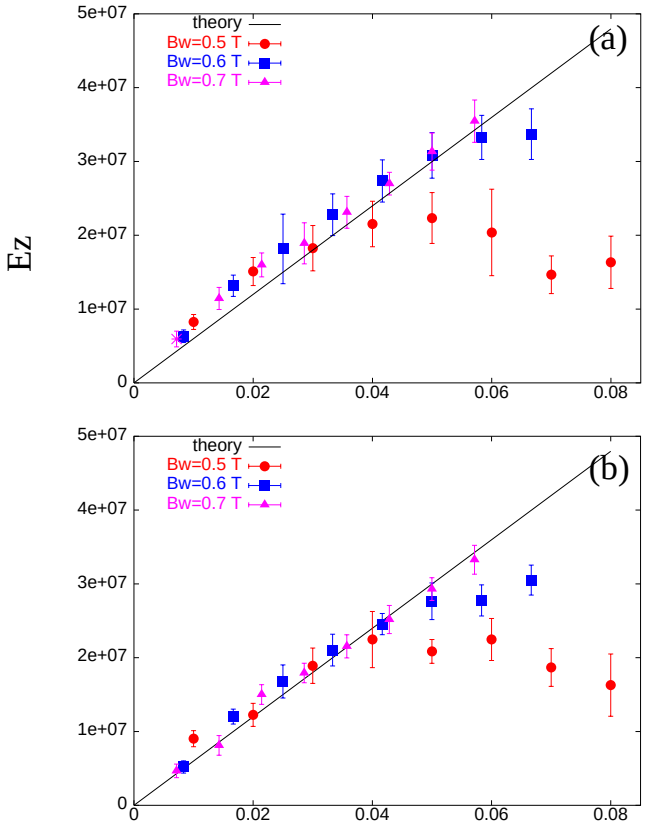

FIGURE 7. E_z vs. $a_1 B_c/B_w$ for (a) $\lambda_w = 0.01$ m and (b) $\lambda_w = 0.02$ m.

A most important figure of merit is the accelerating gradient. As seen in Fig. 5 and Fig. 6, typical values of the accelerating field are of order 10^7 V/m, which are of interest of an ion accelerator. From Eq. (4) and $4\pi J = -\partial E/\partial t$, we calculate the amplitude of the longitudinal field to be

$$E_z = 2B_c \frac{a_1 B_c}{B_w}. \tag{9}$$

For a given value of B_c, E_z is proportional to the product of a_1 and the ratio of B_c to B_w. Figure 7 shows the measured E_z (from simulations) as a function of $a_1 B_c/B_w$ with $B_c = 1$ T. For lower values of $a_1 B_c/B_w$, simulation results agree very well with Eq. (9), but E_z saturates nonlinearly as $a_1 B_c/B_w$ increases. The nonlinearity may be related to the large amplitude of the plasma wave, which is of order $\delta n/n \sim 0.3$ for $a_1 B_c/B_w \sim 0.05$.

SUMMARY

We presented the theory and simulation of EIT in plasma for an electromagnetic pump and a wiggler system. The transparency of the resonant signal is induced by a similar mechanism in both cases. The wiggler system has a couple of desirable properties for an ion accelerator: the phase velocity of the accelerating wave can be controlled and spatially tapered just by tapering of the wiggler. Control of the phase velocity makes it possible to trap and accelerate low energetic heavy particles. We performed a preliminary study of the maximum longitudinal accelerating gradient. Further detailed analysis and simulation is in progress [6].

ACKNOWLEDGMENTS

This work is supported by the US Department of Energy, Division of High-Energy Physics.

REFERENCES

1. A.G. Litvak and M.D. Tokman, Phys. Rev. Lett. **88**, 095003-1 (2002).
2. G. Shvets and J.S. Wurtele, Phys. Rev. Lett. **89**, 115003 (2002).
3. G. Shvets and J.S. Wurtele, Proc. 2002 Advanced Accelerator Concepts.
4. K.J. Boller, A. Imamoglu, and S.E. Harris, Phys. Rev. Lett. **66**, 2593 (1991).
5. S.E. Harris, Phys. Rev. Lett. **70**, 552 (1993).
6. M.S. Hur, J.S. Wurtele, and G. Shvets, in preparation.